

# Dynamic effective mass of granular media

Chaur-Jian Hsu<sup>1</sup>, David Linton Johnson<sup>1</sup>, Nicolas Gland<sup>2</sup>, and Hernán A. Makse<sup>2</sup>

<sup>1</sup> Schlumberger Doll Research, Old Quarry Road, Ridgefield, CT 06877,

<sup>2</sup> Levich Institute and Physics Department, City College of New York, New York, NY 10031.

(Dated: February 19, 2019)

We report an experimental and theoretical investigation of the frequency dependent effective mass,  $\tilde{M}(\omega)$ , of a rigid cavity filled with loose granular particles. We demonstrate the transferability of  $\tilde{M}(\omega)$  to predict the changes in resonant frequency and attenuation for general situations of structure-borne sound. The dominant features of  $\tilde{M}(\omega)$  are a sharp resonance and a broad background which we analyze within the context of simple models as well as with molecular dynamic simulations. We find that: a) These systems may be understood in terms of a height dependent effective sound speed ( $\sim 150$  m/s) and an effective viscosity ( $\sim 2 \times 10^4$  Poise). b) There is a dynamic Janssen effect in the sense that at any frequency, and depending on the method of sample preparation, approximately half the effective mass is borne by the side walls of the cavity and half by the bottom. c) On a fundamental level dissipation is dominated by that at grain-grain contacts, and not by global viscous damping.

PACS Numbers: 45.70.-n, 46.40.-f, 81.05.Rm

Loose grains damp sound very efficiently, and therefore they have been used in many industrial applications where attenuation of sound waves is critical [1, 2]. Furthermore, understanding the mechanisms of energy dissipation via contact dissipative forces between grains is of fundamental interest to unravel the unique dynamical behavior of granular matter. Despite the importance of this problem, an understanding of the origins of damping and dissipation mechanisms in granular materials is still lacking. Moreover, there is a practical motivation to develop an effective method to optimize the damping of unwanted structure borne acoustic signals.

In this Letter we pursue the concept of the effective mass,  $\tilde{M}(\omega)$ , of a granular aggregate contained within a rigid cavity [3]. It is determined by simultaneously measuring the force on the cavity and its acceleration. If, now, an identically filled cavity is located within an acoustically resonant structure, we demonstrate how to predict the shift in resonance frequency and change in Q factor based on a knowledge of  $\tilde{M}(\omega)$ . Generally speaking,  $\tilde{M}(\omega)$  exhibits a sharp resonance, which we interpret in terms of an effective sound speed, and a broad tail decreasing roughly as  $\omega^{-1/2}$ , which we interpret in terms of an effective viscosity. Each of these two interpretations is based on oversimplified toy models, that the entire effective mass is borne by the bottom of the cavity or by the walls, respectively. A concrete example of the former behavior is provided by the effective mass of simple liquids; we demonstrate how our technique enables us to measure the densities and the sound speeds of four different liquids. We have developed molecular dynamic simulations to analyze the expected behavior of  $\tilde{M}(\omega)$  under the assumption that the contacts are described by damped Hertz-Mindlin theory, with or without possible global damping due to the viscosity of the air. We have found that there is a dynamic Janssen effect in the sense that at any frequency approximately half the effective mass rests on the bottom of the cavity and half on the

side walls. Thus, these toy models have only qualitative validity. Notwithstanding, we extract approximate values for the sound speed and the viscosity of our granular ensembles. Finally, our simulations indicate that the dominant microscopic mechanism for damping is at the grain-grain contact level and not due to global viscous damping.

*Experiments.*— We develop the following experimental technique measuring the “effective mass” of the granular material, and we formulate the damping effects of the grains filling cavities of a given structure in terms of the material effective mass. This approach allows us to characterize the granular material over a wide frequency band of sonic interest. A cylindrical cavity of diameter 1.00 in and height 1.21 in excavated in a rigid Al cup is filled with tungsten particles. Each of these particles consists of 4-5 equal-axis particles, of nominal size 100  $\mu\text{m}$ , fused together. We chose tungsten particles because its large density maximizes the effects we are studying. The cup is subjected to an external sinusoidal vibration at angular frequency  $\omega$ ; the resulting acceleration is measured with an accelerometer attached to the cup and the force is measured with a force gauge mounted between the shaker and the cup. The effective mass is defined as the ratio of the total force on the walls of the cavity divided by the acceleration of the rigid cup. Taking into account the mass of the empty cup,  $M_c$ , we have:

$$\tilde{M}(\omega) + M_c = \frac{F(\omega)}{a(\omega)}, \quad (1)$$

where the effective mass of the granular medium,  $\tilde{M}(\omega)$ , is complex-valued, reflecting the partially in-phase, partially out-of-phase motion of the individual grains, relative to the cup motion.

Figure 1 shows our results for a frequency sweep of  $\tilde{M}(\omega)$ . We note that in the low frequency limit  $\tilde{M}(\omega)$  tends to the static mass of the grains, 149 gms. Also, there is a relatively sharp resonance peak around 1.8 kHz

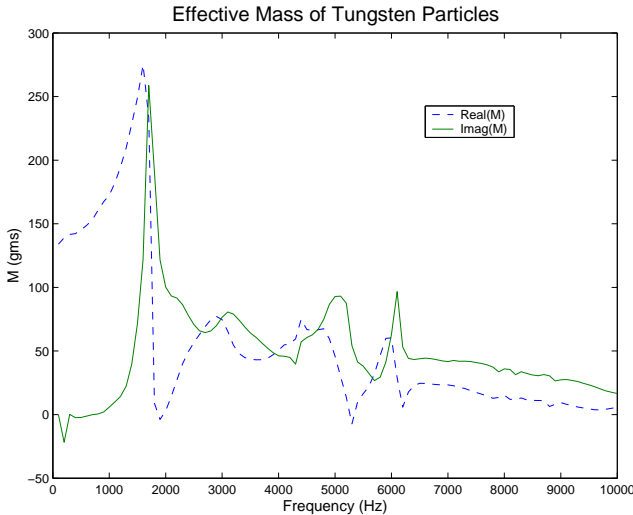


FIG. 1: Effective mass of a cavity filled with 149 gms of Tungsten particle. The resonance frequency is clearly identified.

as well as a broad tail which diminishes with increasing frequency, which we shall discuss.

First, though, we point out the transferability of  $\tilde{M}(\omega)$  to other acoustic experiments, specifically to the damping of acoustic modes. Let us suppose that there is an acoustic structure, possessing an identically shaped cavity, and which has a resonant frequency  $\omega_0$  when the cavity is empty. If one assumes that a) the relevant acoustic wavelengths in the structure are considerably larger than the dimensions of the cup and that b) there is a negligible contribution to the elastic stiffness from the cavity, then, when the cavity is filled with the grains, the density may be thought of as a background density,  $\rho_0$ , plus a localized effective mass due to the grains, viz:

$$\rho(\mathbf{x}) = \rho_0(\mathbf{x}) + \tilde{M}(\omega) \delta^3(\mathbf{x} - \mathbf{x}_1) \quad (2)$$

where the grain-filled cavity is located at position  $\mathbf{x}_1$ . One may re-solve the elasto-dynamic equations to find the new resonant frequency when the cavity is filled. The resonant frequency becomes complex-valued in the presence of the granular damping mechanism:  $\omega = \omega_0 + \Delta\omega$ . For our purposes it is sufficient to consider the results of perturbation theory. We find

$$\Delta\omega = -\frac{\omega_0 \tilde{M}(\omega_0) |\mathbf{u}(\mathbf{x}_1)|^2}{2 \int \rho_0(\mathbf{x}) |\mathbf{u}(\mathbf{x})|^2 dV} \quad (3)$$

where  $\mathbf{u}(\mathbf{x})$  is the displacement field when the cavity is empty of grains. The quality factor is given by  $Q = -\omega_0/[2 \operatorname{Imag}(\Delta\omega)] > 0$ . We have analyzed the predictions of Eq.(3) on a resonant bar made of stainless steel with a grain-filled cavity in the center. When the cavity is empty, the resonant frequency of the lowest flexural mode is  $f_0 = 3019$  Hz and  $Q = 603$ . When the cavity is filled with the tungsten particles there is

a frequency shift,  $\Delta f(\text{exp}) = -77$  Hz, and a very significant increase in damping:  $Q(\text{exp}) = 22$ . The theoretical predictions of Eq.(3) are  $\Delta f(\text{th.}) = -90$  Hz and  $Q(\text{th.}) = 15$ . Of course, there is no guarantee that the two grain-filled cavities are identical, but we take this as significant agreement between theory and experiment in this context. More examples of this sort of comparison will be published elsewhere [4].

On a qualitative level we may understand the general features of Figure 1 in terms of three over-simplified continuum models.

Model I: The granular medium is considered to be a lossy fluid, with negligible viscous effects at the walls i.e. the viscous skin depth  $\delta = \sqrt{2\eta/(\rho\omega)}$  is negligibly small compared to the radius of the cup,  $a$ . Here,  $\eta$  is the viscosity of the fluid,  $\rho$  is the density. The effective mass is simply

$$\tilde{M}(\omega) = \pi a^2 \sqrt{\rho K} \tan(qL)/\omega \quad (4)$$

where  $L$  is the height of the fluid column,  $K = K_0[1 - i\omega\tau]$  is the (lossy) bulk modulus of fluid, and  $q = \omega\sqrt{\rho/K}$  is the wave vector in the fluid. This model predicts that 100% of  $\tilde{M}(\omega)$  is on the bottom surface of the cup and resonance peaks as seen in Figure 2a occur when  $L$  equals odd multiples of a quarter wavelength. The value of  $\tau$  is chosen to match the observed resonance in the experiments. The resonance frequencies are in the ratio 1,3,5,... and the width of the next resonance is nine times as large as the first. So it is scarcely visible on such a plot.

Model II. The granular medium is considered as a very viscous fluid, which is infinitely compressible. Thus, all of  $\tilde{M}(\omega)$  is borne by the walls of the cup, none by the bottom surface. We find:

$$\tilde{M}(\omega) = 2\rho\pi a^2 L J_1(\kappa a)/[\kappa a J_0(\kappa a)]. \quad (5)$$

Here  $\kappa = \sqrt{i\rho\omega/\eta}$  and  $J_k(z)$  is a Bessel function of order  $k$ . This model gives a broad peak with a slow decay at higher frequencies as seen in Figure 2b, much like what is seen, qualitatively, in the granular data away from the fundamental resonance. We note, for future use, that the high frequency limit of Eq.(5) is  $\tilde{M}(\omega) \rightarrow 2\pi a L \sqrt{i\eta\rho/\omega}$ .

Model III. Model II can be used to model an infinitely compressible solid, having a finite, but lossy, shear modulus:  $G = G_0(1 - i\omega\tau)$ . Mathematically, one simply uses Eq.(5) with the substitution  $\eta \rightarrow -iG/\omega$ . With a judicious choice of  $G_0$  and  $\tau$ , Model III also gives a single resonance in the frequency range of interest, similar to Model I. However, as in Model II, in Model III all of  $\tilde{M}(\omega)$  is on the side walls of the cavity.

Note that all three of these models have the same low-frequency asymptote, namely the static mass of the medium:  $\tilde{M}(0) = \rho\pi a^2 L$ . An example of Model I and of Model II are plotted in Figure 2.

A wide variety of real liquids satisfies the assumptions of Model I. We have measured  $\tilde{M}(\omega)$  for four different

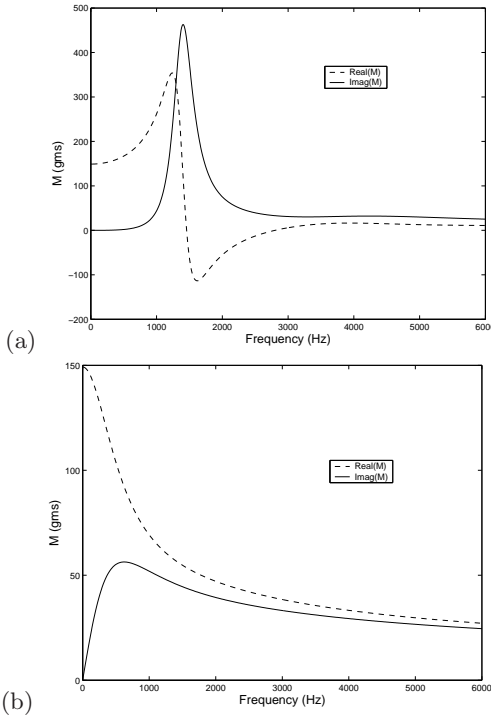


FIG. 2: (a) Model I, a lossy fluid (b) Model II, a highly compressible, highly viscous fluid

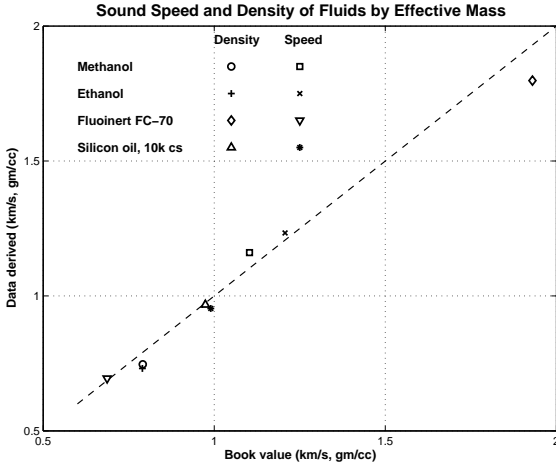


FIG. 3: Crossplot of measured densities (diamonds) and sound speeds (circles) for various fluids.

liquids and they all exhibit the fundamental resonance indicated in Figure 2a. Accordingly, we can extract a value for the sound speed for each fluid. Similarly, from the measured low frequency asymptote we can extract a value for the density. These values measured with our effective mass technique are cross-plot against those determined by more conventional means [5, 6] in Figure 3. Our conclusion is that our technique for measuring the dynamic effective mass  $\tilde{M}(\omega)$  is an accurate one.

Buoyed by these results we naively interpret the main resonance in Figure 1 as being a 1/4 wavelength reso-

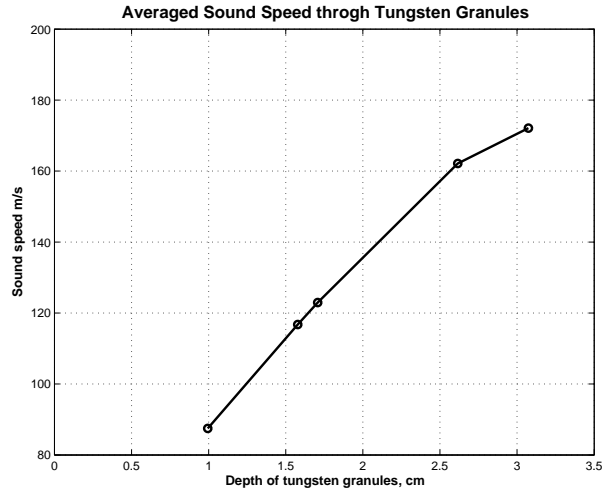


FIG. 4: Effective speed of sound in tungsten granules as a function of filling depth.

nance of the compressional sound speed. We have investigated how this resonance shifts to higher frequencies as the filling depth,  $L$ , is reduced. Throughout the volume of grains in the cup, the sound speed must be depth dependent; the gravity-attributed stiffness is zero at the surface and maximum at the bottom. Nevertheless, we may estimate an effective sound speed in the vertical direction based on this peak frequency and the filling depth of the tungsten particles:

$$v(L) = 4L f_0(L). \quad (6)$$

Figure 4 shows these estimated speeds as a function of filling level. These results show the trend of greater speed with greater depth, as expected. The speed around 170 m/s is also the same order of magnitude as the sound speed in sand grains reported in the literature [1, 3, 7, 8].

In a similar manner we may estimate the effective viscosity of the granular medium based on the high frequency tail of the data, such as in Figure 1. According to Model II the high frequency tail of  $\tilde{M}(\omega)$  should be proportional to  $\omega^{-1/2}$ . Roughly speaking, this is seen in the data plotted in Figure 5 for two different filling levels. Taking into account the prefactors, we conclude that the granular medium has an effective viscosity  $\eta_{\text{eff}} = 1 - 3 \times 10^4$  Poise. Note that this viscosity is *not* the same as what might be relevant for a flow experiment.

The toy models are illuminating as far as they go but to obtain a deeper understanding of the damping mechanism on a microscopic level we have performed molecular dynamic simulations of  $\tilde{M}(\omega)$ . Here, we consider the much simpler system of spherical beads.

In our simulations a static packing at a determined pressure is first achieved by previously determined methods [9], and then we incorporate walls, friction and the force of gravity. The simulations consider the typical Hertz-Mindlin contact forces for the normal and tangential components respectively and the presence of

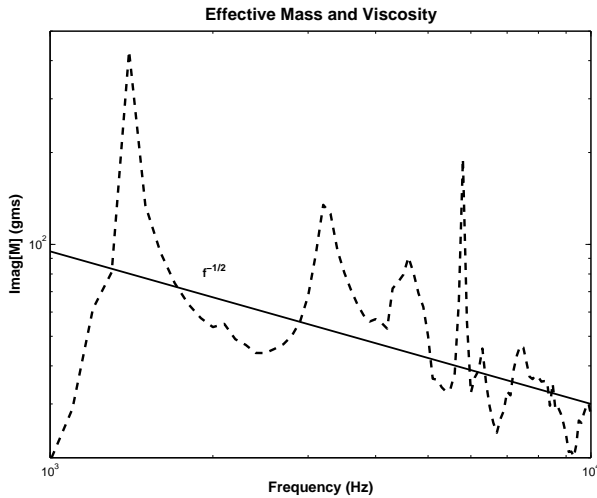


FIG. 5:  $M_2(\omega)$  vs. frequency indicating possible effect of a macroscopic viscosity, for two different filling levels. The feature at 6 kHz is an artifact of our measurement technique.

Coulomb friction between the particle characterized by a friction coefficients  $\mu$ .

Most relevant, microscopic damping is provided by two principal mechanisms of dissipation, described below. If the grains are touching, they exert *contact* damping forces proportional to the relative velocities arising from viscoelastic dissipation in the bulk of the grains:  $f_n^{diss} = -\gamma_n \xi^{1/2} \dot{\xi}$  and  $f_t^{diss} = -\gamma_t \xi^{1/2} \dot{s}$  [10]. Reference values for the damping constants  $\gamma_n$  and  $\gamma_t$  can be obtained from [11]. These damping terms can also model the dissipation arising from liquid bridges at the contact points caused by humidity. (b) A global damping mechanism operates in the form of classical “Rayleigh damping” [12] appropriate to the drag of a sphere immersed in a viscous fluid (which could be also air):  $F^{drag} = 6\pi\eta R\dot{x}$ , where  $\eta$  is the viscosity of the fluid (an analogous expression holds for torque damping) [11, 13].

We apply a sinusoidal oscillation to the external walls of the system and measure the resulting force on the walls and bottom plate to obtain the effective mass of the granular packing for different frequencies and amplitudes of oscillation.

Results are displayed in Fig. 6 for a system in which there is assumed to be only local contact damping. The fundamental resonance and the broad high frequency tail are clearly evident. We show, separately, the contribution to  $\tilde{M}(\omega)$  from the bottom as well as from each of the side walls. The conclusions we draw from the modeling are:

1. A dynamical Janssen effect reveals that Models I, II, and III are equally important to understanding the dynamics. Figure 6a shows the results of the effective mass at the bottom and on the walls of the cavity as a function of the frequency for a system with friction coefficient  $\mu = 0.5$ . For all frequencies we find that approximately

half of the mass is held by the bottom and the other half

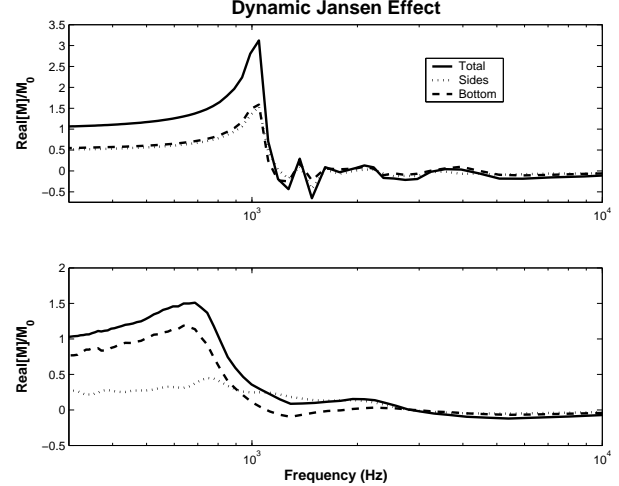


FIG. 6: Computed real part of the effective mass of loose granular media using molecular dynamics simulations vs. frequency: (a) for  $\mu = 0.5$ , (b) for  $\mu = 0$ . Although both simulations clearly show the resonance, in the former approximately half the effective mass is supported by the side walls and half by the bottom.

by the side walls. In this sense, one cannot make the distinction between the simplified Models. Our depiction of an effective sound speed as a function of filling level, Figure 4 is really just a manner of speaking. When the friction is switched off ( $\mu = 0$ , Fig. 6b), almost all the weight is supported by the bottom walls of the cavity, as expected, since the effective shear modulus becomes negligibly small [9] and so Models II and III disappear. (A small component of the weight is held by the walls because they are made of glued particles in the simulations.) Not surprisingly, we still see the resonance peaks as predicted by Model I.

2. Simulations allow us to differentiate between possible different microscopic origins of dissipation. We find that either global or local damping can capture the main features of the experiments: the main resonance peak, as in Model I/III, and a broad high frequency tail, as in Model II. However, the high-frequency asymptotic behavior for large  $\omega$  is very different for the two mechanisms. Global damping predicts  $\tilde{M}(\omega) \sim i\omega^{-1}$ , and this is something we see in our simulations. On the other hand, as long as the viscous skin depth  $\sqrt{2\eta_{eff}/\rho\omega}$  is large compared to the grain size but small compared to the cup radius, then contact damping predicts  $\tilde{M}(\omega) \sim (i/\omega)^{1/2}$ , as in Model II. In Figure 5 we include a plot of  $\tilde{M}(\omega)$  computed from simulations using contact damping only. Although the simulations result is noisy, we may conclude that there is an effective viscosity as for the experimental results. Contact damping can be caused by viscoelasticity of the grains or it can be induced by liquid bridges at the contact points [14].

---

[1] L. Cremer and M. Heckl, *Structure Borne Sound* (Springer, Berlin, 1973).

[2] J. M. Bourinet and D. Le Houedec, *Computers and Structures* **73**, 395 (1999).

[3] J. M. Bourinet and D. Le Houedec, *Powders & Grains* 97 ed. R. Behringer and J. Jenkins Balkema, Rotterdam, 1997.

[4] C.-J. Hsu and D. L. Johnson, (unpublished).

[5] A. Selfridge, *IEEE Trans. Sonics and Ultrasonics* **32** (1985).

[6] Handbook of Chemistry and Physics, 81st Edition (CRC Press, Cleveland, 2000).

[7] C.-h. Liu and S. Nagel, *Phys. Rev. Lett.* **68**, 2301 (1992); C.-h. Liu and S. Nagel, *Phys. Rev. B* **48**, 15646 (1993).

[8] F. D. Shields, J. M. Sabatier and M. Wang, *J. Acoust. Soc. Am.* **108**, 1998 (2000).

[9] H. A. Makse, N. Gland, D. L. Johnson, and L. M. Schwartz, *Phys. Rev. E* **70**, 061302 (2004).

[10] N. V. Brilliantov, F. Spahn, J.-M. Hertzsch, and T. Pöschel, *Phys. Rev E* **53**, 5382 (1996).

[11] J. Schäfer, S. Dippel, and D. E. Wolf, *J. Phys. I* (France) **6**, 5 (1996).

[12] Lord Rayleigh, *Theory of sound*, (Dover Publications, New York, 1945 edition, 1877).

[13] C. Thornton, and D. J. Barnes, *Acta Mechanica* **64**, 45 (1986).

[14] J. N. D'Amour, J. J. R. Stålgren, K. K. Kanazawa, C. W. Frank, M. Rodahl, and D. Johannsmann, *Phys. Rev. Lett.* **96**, 058301 (2006).